

# Expanded Porphyrin-Anion Supramolecular Assemblies: Environmentally Responsive Sensors for Organic Solvents and Anions

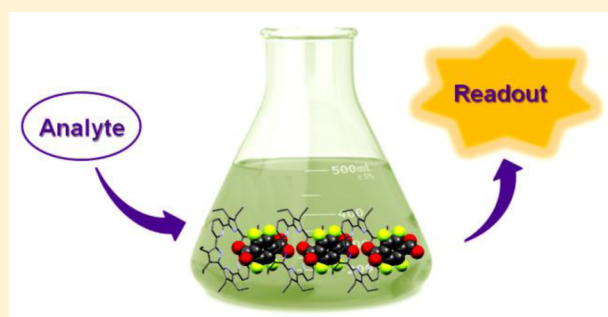
Zhan Zhang,<sup>†</sup> Dong Sub Kim,<sup>†</sup> Chung-Yon Lin,<sup>†</sup> Huacheng Zhang,<sup>†</sup> Aaron D. Lammer,<sup>†</sup> Vincent M. Lynch,<sup>†</sup> Ilya Popov,<sup>‡</sup> Ognjen Š. Miljanić,<sup>‡</sup> Eric V. Anslyn,<sup>\*,†</sup> and Jonathan L. Sessler<sup>\*,†</sup>

<sup>†</sup>Department of Chemistry, The University of Texas at Austin, 105 East 24th Street-Stop A5300, Austin, Texas 78712-1224, United States

<sup>‡</sup>Department of Chemistry, University of Houston, Houston, Texas 77204-5003, United States

## Supporting Information

**ABSTRACT:** Porphyrins have been used frequently to construct supramolecular assemblies. In contrast, noncovalent ensembles derived from expanded porphyrins, larger congeners of naturally occurring tetrapyrrole macrocycles, are all but unknown. Here we report a series of expanded porphyrin-anion supramolecular assemblies. These systems display unique environmentally responsive behavior. Addition of polar organic solvents or common anions to the ensembles leads to either a visible color change, a change in the fluorescence emission features, or differences in solubility. The actual response, which could be followed easily by the naked eye, was found to depend on the specifics of the assembly, as well as the choice of analyte. Using the ensembles of this study, it proved possible to differentiate between common solvents, such as diethyl ether, THF, ethyl acetate, acetone, alcohol, acetonitrile, DMF, and DMSO, identify complex solvent systems, as well as distinguish between the fluoride, chloride, bromide, nitrate, and sulfate anions.



between common solvents, such as diethyl ether, THF, ethyl acetate, acetone, alcohol, acetonitrile, DMF, and DMSO, identify complex solvent systems, as well as distinguish between the fluoride, chloride, bromide, nitrate, and sulfate anions.

## INTRODUCTION

Over the past decade or so, considerable effort has been devoted to the problem of chemosensing.<sup>1,2</sup> Analytical devices and chemical constructs of varying degrees of complexity, including push-pull dyes,<sup>3</sup> fluorescent chromophores,<sup>4</sup> functional polymers,<sup>5-8</sup> and solid metal complexes,<sup>9-12</sup> either used alone or embedded in “artificial noses”,<sup>13-15</sup> have been developed to tell the subtle differences between various small molecules, including solvent vapors. However, sensing common organic solvents in their solution forms remains challenging. Analytical methods, such as HPLC and LC-MS, can provide quantitative data regarding solvent compositions. Unfortunately, such instrumentation-based approaches are not always amenable to use in the field. Thus, there remains a need for chemosensors that allow for the discrimination of solvents. Particularly attractive would be systems that allow for direct, optical-based sensing via simple mixing. Here, we report a new approach to solvent detection based on environmentally responsive, anion-linked supramolecular expanded porphyrin assemblies.

Porphyrins are attractive building blocks for the construction of self-assembled structures. Their planar, conjugated, and rigid structures favor interactions involving  $\pi$ -electrons, including  $\pi$ , $\pi$ -donor-acceptor and  $\pi$ -ion interactions. Porphyrins are also characterized by intense absorption and emission features in the

ultraviolet, visible, and near-infrared spectral regions. The ability of porphyrins to coordinate cations allows for metal-directed self-assembly. To date, porphyrin-based supramolecular assemblies have been studied as promising light-harvesting antennae,<sup>16</sup> chemical sensors,<sup>17</sup> copolymers,<sup>18,19</sup> hosts for planar aromatic guests and fullerenes,<sup>20</sup> as well as hosts capable of recognizing and folding small peptides.<sup>21</sup> When functionalized with hydrogen bond donors/acceptors, porphyrin derivatives have been used to create linear polymers,<sup>16</sup> cyclic oligomers,<sup>22</sup> and cages.<sup>23</sup> In spite of the extensive body of work involving supramolecular porphyrin ensembles, relatively little effort has been devoted to exploring the self-assembly features of their larger congeners, the so-called expanded porphyrins. While the anion-induced dissociation of nonspecific aggregates of sapphyrin,<sup>24</sup> a pentapyrrolic macrocycle, was noted early on, and the self-assembly of hydrophobic derivatives of an octapyrrolic expanded porphyrin, cyclo[8]pyrrole, was used to create liquid crystals,<sup>25</sup> we are unaware of any supramolecular ensembles of expanded porphyrins that have been structurally characterized or whose self-assembly was triggered by the addition of an external guest. As compared to porphyrins, expanded porphyrins typically display distinct optical features,

Received: March 25, 2015

Published: May 12, 2015

more diverse  $\pi$ -conjugation pathways, greater flexibility, and, in many cases, a propensity to interact with anions, as opposed to cations. Here we demonstrate that one representative class of expanded porphyrin, the cyclo[ $m$ ]pyridine[ $n$ ]pyrroles ( $m + n = 6$ ), may be used to stabilize a new class of anion-derived self-assembled constructs whose environmentally responsive behavior makes them attractive as chemical sensors for both common solvents and anionic analytes under conditions of simple mixing.

To date, anions have been extensively explored in the context of supramolecular self-assembly. One prominent and well-recognized role of anions is as templates to construct elaborate, multicomponent structures,<sup>26,27</sup> including mechanically interlocked motifs, such as rotaxanes, pseudorotaxanes, and catenanes.<sup>28–31</sup> Anions have also been used directly as building blocks to create supramolecular ensembles.<sup>32–37</sup> Perhaps as the result of weak binding interactions involved, most of the latter systems have only been characterized in the solid state, with only a few actually studied in solution.<sup>36,37</sup> In the case of the 1:1 self-assembled materials produced from the expanded porphyrins of the present study, standard isodesmic analyses reveal evidence for strong anion binding in chloroform. Nevertheless, these and the related 1:2 ensembles undergo a change in structure when exposed to polar solvents and Lewis basic anions. The resulting analyte-induced changes are manifest in terms of differences in color, solubility, and fluorescence emission intensity that may be easily monitored by the unaided eye. This makes the present constructs useful as chemical sensors. To the best of our knowledge, these assemblies are the only known supramolecular systems that can be used to differentiate at least eight different solvents and five types of anions by simple optical means.

## RESULTS AND DISCUSSION

**Design and Preparation of the Supramolecular Assemblies.** Cyclo[ $m$ ]pyridine[ $n$ ]pyrroles ( $P_mP_n$ ) are pyridine-containing analogues of cyclo[6]pyrroles.<sup>38</sup> Protonation of these nonaromatic macrocycles can lead to the expansion of  $\pi$ -conjugation and, in the case of cyclo[2]pyridine[4]pyrrole ( $P_2P_4$ ), the global delocalization of the  $\pi$ -electrons. Notably the diprotonated forms of cyclo[3]pyridine[3]pyrrole ( $P_3P_3$ ) and  $P_2P_4$ , including  $P_3P_3$ -2TFA,  $P_2P_4$ -2TFA,  $P_2P_4$ -2MSA, and  $P_2P_4$ -2HCl, share a similar structural feature in solid state: The two counteranions reside separately on the two sides of the macrocycles.<sup>39</sup> This observation led us to consider that it might be possible to synthesize linear supramolecular polymers using these macrocycles in conjunction with suitable diacids (Figure 1). Since protonation is required for anion binding and hence is a prerequisite for the formation of the putative assemblies, weak acids that cannot protonate these macrocycles were not expected to promote self-assembly. In fact, little evidence of protonation or self-assembly was observed when either  $P_2P_4$  or  $P_3P_3$  was mixed with terephthalic acid ( $pK_a = 4.2$ ). Stronger diacids, specifically 4,4'-biphenyldisulfonic acid (BPDSA,  $pK_{a1} = -3.0$ ), tetrafluoroterephthalic acid (TFTPA,  $pK_{a1} = \text{ca. } 1.0$ ), octafluorobiphenyldicarboxylic acid (OFBPA,  $pK_{a1} = \text{ca. } 1.0$ ),<sup>40</sup> oxalic acid (OA,  $pK_{a1} = 1.2$ ), and acetylene dicarboxylic acid (ADCA,  $pK_{a1} = 0.7$ ) were thus explored as potentially more suitable building blocks.

As an initial test of whether anion-induced self-assembly would occur,  $P_2P_4$  (0.2 M) in  $\text{CH}_2\text{Cl}_2$  (50 mL) was treated with an excess of BPDSA dissolved in a trace quantity of methanol (0.1 mL). An instant color change was observed,

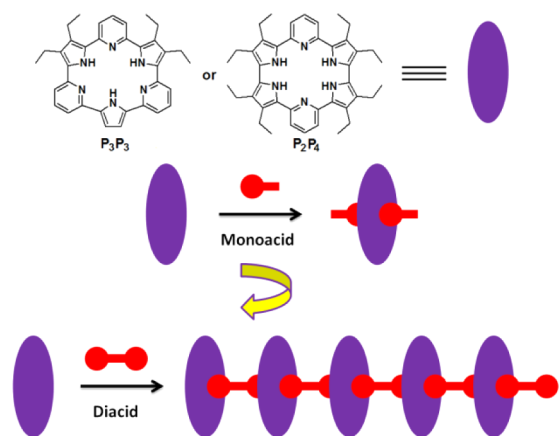


**Figure 1.** Design of anion-linked supramolecular assemblies based on  $P_3P_3$  and  $P_2P_4$ .

along with the subsequent formation of a fluffy suspension. This was taken as an indication that protonation and aggregation were occurring under these reaction conditions. Similar changes were observed when TFTPA or OFBPA were used. On the other hand, mixing OA or ADCA with  $P_3P_3$  or  $P_2P_4$  under similar conditions yielded transparent solutions, albeit ones characterized by dramatic color changes. When more concentrated solutions (2 M) of these latter acids were used, precipitation occurred. In light of these observations, the  $P_mP_n$ -diacid supramolecular assemblies were obtained by sonicating the macrocycle and a selected acid in  $\text{CH}_2\text{Cl}_2$ .

**Solid-State Characterization.** Single crystals of the solid materials were obtained using slow diffusion or vapor diffusion methods (cf. Supporting Information). X-ray crystallographic analysis revealed the formation of infinitely repeating supramolecular assemblies in the solid state. These structures were characterized by either a 1:1 or 1:2 macrocycle-to-anion ratio, depending on the anion and expanded porphyrin in question (Figure 2). For instance, BPDSA, TFTPA, and OFBPA gave rise to assemblies characterized by 1:1 binding stoichiometries. In contrast, the use of OA or ADCA led to the formation of 1:2 assemblies. The change in binding stoichiometry is rationalized in terms of the acidity of the corresponding acid. For instance, the first and second  $pK_a$  values of OA are 1.2 and 4.1, respectively. The low  $pK_{a1}$  value enables oxalic acid to protonate a first  $P_mP_n$  macrocycle readily. However, the relatively high value of  $pK_{a2}$  value precludes protonation of a second macrocycle. Consequently each diprotonated macrocycle becomes capped by two monoanions. Ensembles with a 1:2 stoichiometry are then stabilized as the result of hydrogen bonding interactions between the remaining (i.e., protonated) carboxyl groups. In contrast, the  $pK_{a2}$  values for BPDSA and TFTPA are around 2.0 (cf. Supporting Information). As a result, one molecule of acid can protonate two macrocycles giving rise to self-assembled oligomers of 1:1 stoichiometry.

Depending on the choice of macrocycle and anion, 1:1 assemblies with either linear or zigzag structures are seen in the solid state. For example, the  $P_3P_3$ -BPDSA,  $P_3P_3$ -TFTPA, and  $P_2P_4$ -OFBPA ensembles exhibit a zigzag structure, while  $P_2P_4$ -TFTPA crystallizes in the form of an orderly linear structure (Figure 2). In the case of the 1:1 ensemble,  $P_3P_3$ -TFTPA, additional acid molecules are present in the crystal lattice, which serve to link the strands into a 2D network (Supporting Information, Figure S14). Such a solid state cross-linking phenomenon is observed in the case of most of the 1:2

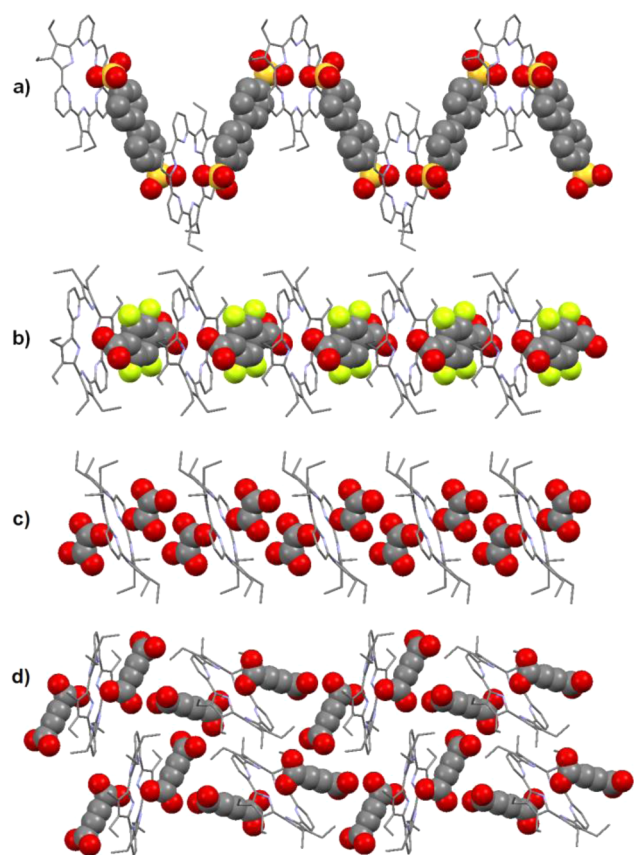


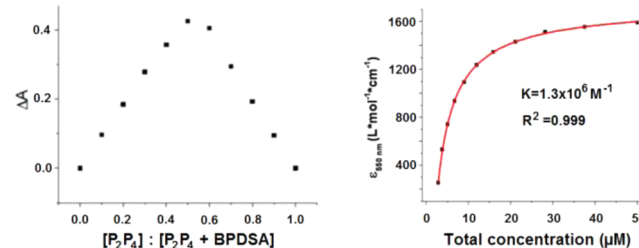
**Figure 2.** Truncated views of the X-ray diffraction structures of the extended supramolecular ensembles seen in the solid state: (a)  $P_3P_3$ -BPDSA; (b)  $P_2P_4$ -TFTPA; (c)  $P_2P_4$ -OA; and (d)  $P_2P_4$ -ADCA.

assemblies reported here. In fact, except for assembly  $P_2P_4$ -OA, which is characterized by a 1D linear structure, all the other 1:2 assemblies characterized by X-ray diffraction analysis were found to exist in the form of 2D or 3D hydrogen bonding networks, with either acid or solvent molecules being found to link the repeating subunits. In the case of  $P_2P_4$ -ADCA (Figure 2d), hydrogen bonding between the unreacted carboxyl groups serve to link the assembly into a 2D grid-like network. In the case of  $P_3P_3$ -ADCA (Supporting Information, Figure S15), a 3D network is stabilized by water molecules when analogous crystals were grown in the presence of undried THF. On the basis of these single crystal structures, the average distance between the NH protons and the closest oxygen is around 2.4 Å. Such a short separation is consistent with strong hydrogen bonding interactions between the protonated macrocycles and the anions. In the case of the 1:1 structures,  $P_3P_3$ -BPDSA,  $P_mP_n$ -TFTPA, and  $P_mP_n$ -OFBPA, the macrocycle is roughly 3.3–3.7 Å away from the closed aromatic ring of the dicarboxylate counteranion. This finding leads us to suggest that  $\pi$ , $\pi$ -donor–acceptor interactions may also play a role in stabilizing these assemblies. Interestingly, in order to achieve efficient packing of the  $P_3P_3$ -BPDSA assembly, the biphenyl group within the BPDSA subunit adopts an unusual pseudoplanar conformation in the solid state.

In order to determine the morphology of the ensembles produced under conditions of fast evaporation, rather than slow crystallization, drop-cast samples were prepared and studied by scanning electron microscope (SEM). Toward this end, a dilute dichloromethane solution of the ensemble in question was

placed on a clean aluminum foil and allowed to evaporate under ambient conditions. The microcrystalline material that resulted was examined by SEM. Long needle-shaped microstructures were observed in all cases. The length of the needles was in the range of roughly 10–50  $\mu\text{m}$  for the less soluble 1:1 polymers. Longer and wider structures were observed for the more soluble 1:2 assemblies. For instance, in the case of  $P_2P_4$ -ADCA, well-defined, 300  $\mu\text{m}$ -long needle-like structures were observed (Supporting Information, Figure S4). In all cases, the general morphology of the microcrystals proved similar to the corresponding single crystals used for the X-ray diffraction analyses.

**Solution-State Binding Studies.** Several of the supramolecular aggregates described above proved amenable to study in solution. In all cases where reliable analyses could be carried out, the findings proved consistent with the solid state structures. For instance, Job plots of  $P_3P_3$ -BPDSA and  $P_2P_4$ -BPDSA as recorded in chloroform containing a trace of methanol supported a 1:1 binding stoichiometry (Figure 3 and



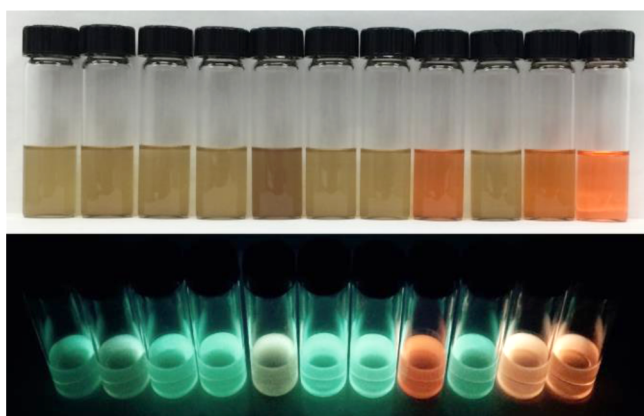
**Figure 3.** Solution-state analyses of the supramolecular ensemble formed from  $P_2P_4$  and BPDSA. Left: continuous variation plot for a 1:1 mixture of  $P_2P_4$  and BPDSA. These plots were constructed by plotting the product of the absorption change at 451 nm and the mole fraction of  $P_2P_4$  vs the mole fraction of  $P_2P_4$  and BPDSA. Right: Plot of molar extinction coefficient as a function of the total concentration of an equimolar mixture of  $P_2P_4$  and BPDSA.

Figure S5). Likewise, Job plots of  $P_2P_4$ -OA were consistent with a 1:2 binding stoichiometry. Unfortunately, in the case of  $P_3P_3$ -OA, as well as the TFTPA- and OFBPA-derived assemblies, the binding stoichiometry in solution could not be established because the absorption changes were too small to allow for the construction of reliable Job plots.

To determine the binding affinities corresponding to the interaction between the  $P_mP_n$  macrocycles of this study and the various anions tested in solution, plots of the extinction coefficients as a function of total concentration of  $P_3P_3$ -BPDSA or  $P_2P_4$ -BPDSA were constructed. The putative binding constants were calculated based on a modified equal K fitting approach.<sup>41</sup> Nonlinear curve-fitting analysis using an isodesmic model<sup>41–43</sup> gave a binding constant of  $1.3 \times 10^6 \text{ M}^{-1}$  for  $P_2P_4$ -BPDSA and  $2.2 \times 10^5 \text{ M}^{-1}$  for  $P_3P_3$ -BPDSA in chloroform containing a trace of methanol. According to the same model, the  $P_2P_4$ -BPDSA assembly exists as an average 6-mer at a total concentration of 50  $\mu\text{M}$ , which represents the solubility limit. Although the modest nature of the spectral shifts precluded Job plot determinations (vide supra), good fits were obtained when the isodesmic model was applied to extinction coefficient studies involving the  $P_3P_3$ -TFTPA and  $P_2P_4$ -TFTPA systems. We take this as evidence that a 1:1 binding mode pertains for these ensembles in solution, as well as in the solid state. In pure chloroform, binding constants of  $2.0 \times 10^6$  and  $8.1 \times 10^5 \text{ M}^{-1}$  were determined for  $P_2P_4$ -TFTPA and  $P_3P_3$ -TFTPA, respec-

tively. These high binding affinities are ascribed to a combination of hydrogen bonding, Coulomb forces, and  $\pi,\pi$  donor–acceptor interactions, as would be inferred from an analysis of the solid state structures. In contrast, hydrogen bonding appeared to be the only tethering interaction within the repeat units (anion–macrocycle–anion) that make up the 1:2 assemblies. This could account for the higher solubility of these latter systems relative to the 1:1 assemblies.

**Solvent Response.** These supramolecular assemblies were found to respond to various solvents, including diethyl ether, THF, ethyl acetate, acetone, methanol, acetonitrile, DMF, and DMSO. Upon the addition of 10% v.v. of such polar solvents to the ensembles in  $\text{CH}_2\text{Cl}_2$ , either a change in color, solubility, or fluorescence of the ensembles is observed. In the case of  $\text{P}_3\text{P}_3\text{-BPDSA}$ , for instance (Figure 4), addition of THF converted



**Figure 4.** Solvent response observed for the  $\text{P}_3\text{P}_3\text{-BPDSA}$  assembly. 10% v. v. of polar solvents were added to a  $\text{CH}_2\text{Cl}_2$  solution of the assembly. Top: color changes; bottom: fluorescence changes. From left to right: control (only  $\text{CH}_2\text{Cl}_2$ ), chloroform, toluene, diethyl ether, THF, ethyl acetate, acetone, methanol, acetonitrile, DMF, and DMSO.

the initial light brown, fluffy suspension into a dark brown suspension, while the addition of methanol, DMF, and DMSO served to convert the suspension into a clear red solution. The sample containing THF was found to give rise to a gray fluorescence emission, while the methanol sample produced an intense red fluorescence and the DMF and DMSO samples gave a light red fluorescence when excited at 365 nm. As such, this ensemble permits THF and methanol to be identified uniquely. In an analogous manner,  $\text{P}_2\text{P}_4\text{-OA}$  could be used to identify acetone uniquely, while acetonitrile could be determined selectively using  $\text{P}_3\text{P}_3\text{-OA}$  or  $\text{P}_3\text{P}_3\text{-ADCA}$  and DMSO using  $\text{P}_2\text{P}_4\text{-BPDSA}$  or  $\text{P}_2\text{P}_4\text{-ADCA}$ . In these ensembles, methanol led to a quenching of the fluorescence. However, no effective distinction between methanol and ethanol could be made. On the other hand, by analyzing the response across several assembly systems, we could also identify diethyl ether, ethyl acetate, and DMF within the test group of solvents. Unfortunately, the present assemblies are non-responsive toward relatively less polar solvents, such as chloroform, toluene, and benzene. The responses we do see in the case of the more polar solvents reflects, presumably, competition for hydrogen bonding sites and changes in the extent of protonation/deprotonation. These differences affect the degree of interaction between the expanded porphyrin and the dianions (or their conjugate acid forms), as well as the extent of aggregation (Scheme 1).

### Scheme 1. Proposed Structural Changes That Occur When the Assemblies of This Study Are Exposed to Polar Solvents

Supramolecular Assemblies  $\xrightarrow{\text{Polar solvent}}$  Shorter Assemblies + Monomers

The ability of these expanded porphyrin-diacid pairs to differentiate complex solvent systems was further explored by studying their cross-reactivity. Toward this end, discrimination experiments were carried out using four assemblies ( $\text{P}_3\text{P}_3\text{-BPDSA}$ ,  $\text{P}_2\text{P}_4\text{-BPDSA}$ ,  $\text{P}_2\text{P}_4\text{-ADCA}$ , and  $\text{P}_3\text{P}_3\text{-TFTPA}$ ). Each assembly (1.0 mM in  $\text{CH}_2\text{Cl}_2$ , 100  $\mu\text{L}$ ) was subjected to 32 different solvent mixtures, each composed of two solvents, either acetonitrile, chloroform, benzene, or toluene (100  $\mu\text{L}$ ) mixed with diethyl ether, THF, ethyl acetate, acetone, methanol, ethanol, DMF, or DMSO (10  $\mu\text{L}$ ). The fluorescence response for each assembly and solvent mixture was recorded (490–690 nm, 20 nm increments) and subject to linear discriminate analysis (LDA) using the XLSTAT suite, Figure 5. This resulted in a cross-validation classification accuracy of 86.5%.

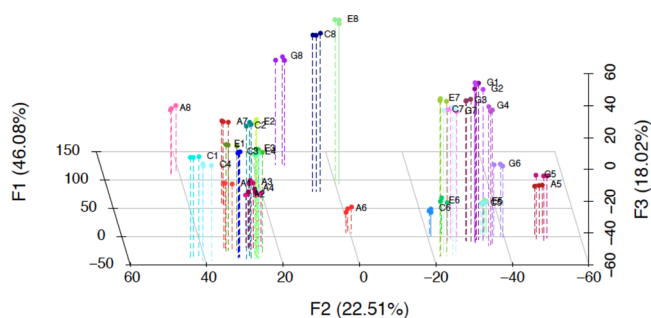


**Figure 5.** Three-dimensional LDA score plot of the fluorescence response. Four assemblies ( $\text{P}_3\text{P}_3\text{-BPDSA}$ ,  $\text{P}_2\text{P}_4\text{-BPDSA}$ ,  $\text{P}_2\text{P}_4\text{-ADCA}$ , and  $\text{P}_3\text{P}_3\text{-TFTPA}$ ) were exposed to 32 different solvent mixtures. Solvent mixtures are coded with one letter representing acetonitrile (A), toluene (C), benzene (G), or chloroform (E) and one number representing diethyl ether (1), THF (2), ethyl acetate (3), acetone (4), methanol (5), ethanol (6), DMF (7), and DMSO (8).

In contrast to the relatively dramatic optical changes observed upon exposure of the assemblies to single solvents, the fluorescence changes produced in response to different solvent mixtures were subtle and nonspecific. Thus, linear discriminate analysis (LDA) was employed to recognize and classify the unique fluorescence change patterns obtained when the various assemblies were challenged with different solvent mixtures. In this way, relatively good differentiation was obtained in most cases, as noted above. The solvents mixtures that overlapped contained either THF or ether at the 10% concentration (v./v.) level in benzene or toluene, or reflected sheer coincidence. A particularly attractive feature of the expanded porphyrin-diacid array approach detailed here is that the variance is distributed along many axes, creating a 4-dimensional space. This multiaxis variance reflects a high level of cross-reactivity<sup>44</sup> and demonstrates the potential for these self-assembled systems as chemosensors to differentiate subtly different and complex solvent mixtures. Efforts to quantify this response are ongoing.

**Anion Response.** Because appropriately chosen anions could compete with the carboxylate guests for the protonated expanded porphyrin sites, small Lewis basic anions were tested as potential analytes. A remarkable response was observed. In

the case of the  $P_2P_4$ -BPDSA ensemble, for instance, fluoride, chloride, bromide, iodide, nitrate, sulfate, monobasic phosphate, but not iodide (all studied in the form of their solid tetrabutylammonium (TBA) or tetramethylammonium (TMA) salts) produced an optical response (Supporting Information, Figure S28). With this system, the addition of fluoride and monobasic phosphate served to dissolve the fluffy suspension and reduce the color of the solution. Addition of chloride also led to the instantaneous (on the laboratory time scale) production of a transparent solution that was darker in color than the original suspension. Although no obvious change in color was seen upon treating with nitrate or sulfate, it was found that nitrate quenched the fluorescence, while the sample with sulfate gave rise to a blue fluorescence. Interestingly, time was required for an appreciable degree of solubilization to occur in the case of bromide and nitrate. After 1 h, a clear dark brown solution or a bright yellow solution was produced in the case of bromide and nitrate, respectively. The samples containing chloride or bromide produced a weak yellow emission, while monobasic phosphate produced a bright fluorescence and fluoride gave an intense yellow emission. Therefore, using only  $P_2P_4$ -BPDSA we were able to identify at least five anions. The other ensembles gave rise to different response patterns. For instance, the fluoride anion produced a bright fluorescence in the case of all the  $P_2P_4$ -diacid systems but not the  $P_3P_3$ -diacid ones. On the other hand, chloride gave rise to visible color changes in the case of the  $P_mP_n$ -BPDSA,  $P_mP_n$ -OFBPA, and  $P_mP_n$ -ADCA ensembles.

## CONCLUSIONS

In summary, we have successfully synthesized a series of expanded porphyrin-anion supramolecular assemblies using  $P_mP_n$  macrocycles and diacids. These assemblies are characterized by highly ordered structures in the solid state. In the case of the 1:1 complexes where the isodesmic model could be applied successfully for analysis, strong interactions between the macrocycle and the various test anions were observed. The self-assembled systems reported here are environmentally responsive and undergo distinct changes in solubility, color, and fluorescence intensity when exposed to polar solvents or Lewis basic anions. The responses differ from ensemble to ensemble and from analyte to analyte. Using cross-reactivity discrimination analyses, these systems were found capable of differentiate complex solvent systems. We thus propose that the present systems may have a role to play as chemosensors that allow certain salts and various solvents to be identified easily by optical or visual means. In preliminary work, we have also found that the present ensembles respond to solvent vapors. This aspect of the chemistry, as well as efforts to quantify the solution-based response, are currently ongoing.

## ASSOCIATED CONTENT

### Supporting Information

Synthetic experimental, additional spectroscopic information, structural data, and theory calculations. The Supporting Information is available free of charge on the ACS Publications website at DOI: 10.1021/jacs.5b03131.

## AUTHOR INFORMATION

### Corresponding Authors

\*anslyn@austin.utexas.edu

\*sessler@cm.utexas.edu

## Notes

The authors declare no competing financial interest.

## ACKNOWLEDGMENTS

This research was supported by the U.S. National Science Foundation (Grant CHE-1151292 to O.S.M.), the National Institutes of Health (Grants CA 068682 and GM 065515 to J.L.S. and E.V. A., respectively) and Welch Foundation (Grants F-1018 and E-1768 to J.L.S. and O.S.M., respectively). O.S.M. is a Cottrell Scholar of the Research Corporation for Science Advancement.

## REFERENCES

- (1) Zhou, X.; Lee, S.; Xu, Z.; Yoon, J. *Chem. Rev.* **2015**, *115*, ASAP. DOI: 10.1021/cr500567r.
- (2) Askim, J. R.; Mahmoudi, M.; Suslick, K. S. *Chem. Soc. Rev.* **2013**, *42*, 8649–8682.
- (3) Reichart, C. *Chem. Rev.* **1994**, *94*, 2319–2358.
- (4) Li, J.; Hu, G.; Li, X.; Hu, B.; Wang, N.; Lu, P.; Wang, Y. *Eur. J. Org. Chem.* **2013**, 7320–7327.
- (5) Peterson, J. J.; Davis, A. R.; Werre, M.; Coughlin, E. B.; Carter, K. R. *ACS Appl. Mater. Interfaces* **2011**, *3*, 1796–1799.
- (6) Kumari, P.; Bera, M. K.; Malik, S.; Kuila, K. *ACS Appl. Mater. Interfaces* **2015**, *7*, ASAP. DOI: 10.1021/am507266e.
- (7) Yoon, J.; Chae, S. K.; Kim, J.-M. *J. Am. Chem. Soc.* **2007**, *129*, 3038–3039.
- (8) Freund, M. S.; Lewis, N. S. *Proc. Natl. Aca. Sci. U.S.A.* **1995**, *92*, 2652–2656.
- (9) Qin, L.; Zheng, M.-X.; Guo, Z.-J.; Zheng, H.-G.; Xu, Y. *Chem. Commun.* **2015**, *51*, 2447–2449.
- (10) Wang, D.; Zhang, L.; Li, G.; Huo, Q.; Liu, Y. *RSC Adv.* **2015**, *5*, 18087–18091.
- (11) Saha, A.; Panos, Z.; Hanna, T.; Huang, K.; Hernández-Rivera, M.; Martí, A. A. *Angew. Chem., Int. Ed.* **2013**, *52*, 12615–12618.
- (12) Mansour, M. A.; Connick, W. B.; Lachicotte, R. J.; Gysling, H. J.; Eisenberg, R. *J. Am. Chem. Soc.* **1998**, *120*, 1329–1330.
- (13) Rankin, J. M.; Zhang, Q.; LaGasse, M. K.; Zhang, Y.; Askim, J. R.; Suslick, K. S. *Analyst* **2015**, *140*, 2613–2617.
- (14) Lin, H.; Jang, M.; Suslick, K. S. *J. Am. Chem. Soc.* **2011**, *133*, 16786–16789.
- (15) Rakow, N. A.; Suslick, K. S. *Nature* **2000**, *406*, 710–713.
- (16) Drain, C. M. *Proc. Natl. Aca. Sci. U.S.A.* **2002**, *99*, 5178–5182.
- (17) Purrello, R.; Gurrieri, S.; Lauceri, R. *Coord. Chem. Rev.* **1999**, *683*–706.
- (18) Kubo, Y.; Kitada, Y.; Wakabayashi, R.; Kishida, T.; Ayabe, M.; Kaneko, K.; Takeuchi, M.; Shinkai, S. *Angew. Chem., Int. Ed.* **2006**, *45*, 1548–1553.
- (19) Twyman, L. J.; King, A. S. H. *Chem. Commun.* **2002**, 910–911.
- (20) Meng, W.; Breiner, B.; Rissanen, K.; Thoburn, J. D.; Clegg, J. K.; Nitschke, J. R. *Angew. Chem., Int. Ed.* **2011**, *50*, 3479–3783.
- (21) Tashiro, S.; Kobayashi, M.; Fujita, M. *J. Am. Chem. Soc.* **2006**, *128*, 9280–9281.
- (22) Ohkawa, H.; Takayama, A.; Nakajima, S.; Nishide, H. *Org. Lett.* **2006**, *8*, 2225–2228.
- (23) Singh, S.; Aggarwal, A.; Farley, C.; Hageman, B. A.; Batteas, J. D.; Drain, C. M. *Chem. Commun.* **2011**, *47*, 7134–7136.
- (24) Sessler, J. L.; Andrievsky, A.; Gale, P. A.; Lynch, V. *Angew. Chem., Int. Ed.* **1996**, *35*, 2782–2785.
- (25) Stepien, M.; Donnio, B.; Sessler, J. L. *Angew. Chem., Int. Ed.* **2007**, *46*, 1431–1435.
- (26) Hasenkopf, B.; Lehn, J. M.; Kniesel, B. O.; Baum, G.; Fenske, D. *Angew. Chem., Int. Ed.* **1996**, *35*, 1838–1840.
- (27) Hasenkopf, B.; Lehn, J. M.; Boumediene, N.; Dupont-Gervais, A.; van Dorsselaar, A.; Kniesel, B.; Fenske, D. *J. Am. Chem. Soc.* **1997**, *119*, 10956–10962.
- (28) Fyfe, M. C. T.; Glink, P. T.; Menzer, S.; Stoddart, J. F.; White, A. J. P.; Williams, D. J. *Angew. Chem., Int. Ed. Engl.* **1997**, *36*, 2068–2070.

- (29) Wisner, J. A.; Beer, P. D.; Drew, M. G. B. *Angew. Chem., Int. Ed.* **2001**, *40*, 3606–3609.
- (30) Hübner, G. M.; Gläser, J.; Seel, C.; Vögtle, F. *Angew. Chem., Int. Ed.* **1999**, *38*, 383–386.
- (31) Mullen, K. M.; Beer, P. D. *Chem. Soc. Rev.* **2009**, *38*, 1701–1713.
- (32) Hosseini, M. W.; Ruppert, R.; Schaffer, P.; DeCian, A.; Kyritsaka, N.; Fischer, J. *J. Chem. Soc., Chem. Commun.* **1994**, 2135–2136.
- (33) Hosseini, M. W.; Brand, G.; Schaeffer, P.; Ruppert, R.; De Cian, A.; Fischer, J. *Tetrahedron Lett.* **1996**, *37*, 1405–1408.
- (34) Maeda, H.; Kusunose, Y. *Chem.—Eur. J.* **2005**, *11*, 5661–5666.
- (35) Metrangolo, P.; Meyer, F.; Pilati, T.; Resnati, G.; Terraneo, G. *Chem. Commun.* **2008**, 1635–1637.
- (36) Wang, T.; Yan, X.-P. *Chem.—Eur. J.* **2010**, *16*, 4639–4649.
- (37) Gong, H.-Y.; Rambo, B. M.; Karnas, E.; Lynch, V. M.; Sessler, J. L. *Nat. Chem.* **2010**, *2*, 406–409.
- (38) Köhler, T.; Seidel, D.; Lynch, V.; Arp, F. O.; Ou, Z.; Kadish, K. M.; Sessler, J. L. *J. Am. Chem. Soc.* **2003**, *125*, 6872–6873.
- (39) Zhang, Z.; Lim, J. M.; Ishida, M.; Roznyatovskiy, V. V.; Lynch, V. M.; Gong, H.-Y.; Yang, X.; Kim, D.; Sessler, J. L. *J. Am. Chem. Soc.* **2012**, *134*, 4076–4079.
- (40) Chen, T.-H.; Popov, I.; Zenasni, O.; Daugulis, O.; Miljanić, O. Š. *Chem. Commun.* **2013**, *49*, 6846–6848.
- (41) Park, J. S.; Yoon, K. Y.; Kim, D. S.; Lynch, V. M.; Bielawski, C. W.; Johnston, K. P.; Sessler, J. L. *Proc. Natl. Acad. Sci. U. S. A.* **2011**, *108*, 20913–20917.
- (42) Martin, R. B. *Chem. Rev.* **1996**, *96*, 3043–3064.
- (43) Brunsveld, L.; Folmer, B. J. B.; Meijer, E. W.; Sijbesma, R. P. *Chem. Rev.* **2001**, *101*, 4071–4098.
- (44) Stewart, S.; Adams, M.; Anslyn, E. V. *Chem. Soc. Rev.* **2014**, *43*, 70–84.